We are IntechOpen,
the world's leading publisher of Open Access books
Built by scientists, for scientists

6,900
Open access books available

186,000
International authors and editors

200M
Downloads

Our authors are among the

154
Countries delivered to

TOP 1%
most cited scientists

12.2%
Contributors from top 500 universities

BOOK CITATION INDEX
CLARIVATE ANALYTICS
INDEXED

WEB OF SCIENCE™

Selection of our books indexed in the Book Citation Index
in Web of Science™ Core Collection (BKCI)

Interested in publishing with us?
Contact book.department@intechopen.com

Numbers displayed above are based on latest data collected.
For more information visit www.intechopen.com

Energy Efficient Control of Fans in Ventilation Systems

Bjørn R. Sørensen

Additional information is available at the end of the chapter

http://dx.doi.org/10.5772/48597

1. Introduction

Ventilation fans are energy-demanding equipment that stands for a significant share of a building's total energy consumption. Improving energy efficiency of ventilation fans is thus important. Fans used for demand controlled ventilation (DCV) are intended to deliver a specific flow rate derived from the actual load in the building. This chapter is about how to deliver the required air flow rate to all rooms, without wasting energy on throttling. There are several ways to control the flow rate in a ventilation system. The most common ways are (1) pure throttling, (2) constant differential pressure and (3) constant duct static pressure. In some situations, (4) direct fan control are used as a control strategy (DDCV). The latter is known to be efficient, as it will provide only the required air flow at all times, without the need for any throttling. It needs however more extensive instrumentation, and flow rates to and from all zones in a building have to be continually recorded and fed back to the central flow controller. A simulation study shows that by introducing a relatively simple control procedure, the fan can be controlled more efficient and energy consumption can be reduced to a significant degree, also for alternative (2) and (3), without the need for added control equipment.

Pressure energy used for throttling of air in the ventilation system is transformed to heat by friction. Thus the ventilation air is heated by the 'wasted' pressure energy. For this reason it can be argued that throttling is just as good as pure speed regulation. However, this makes sense only if a demand for heating exists. During periods with cooling demands, throttling is a true waste of energy since the heat produced from it cannot be exploited. If there is local cooling of air within the zones, throttling is even worse since energy must be used to remove the 'throttling' heat. Throttling also produces noise. Hence, the degree of throttling in ventilation systems should be as low as possible.

In this study a different approach of controlling the static pressure difference of a fan is suggested. The study is based on a detailed dynamic simulation system that was presented in (Sørensen, 2006, 2010). Controlling static pressure difference of the fan to a fixed set point is a compromise between pure throttling and pure speed regulation. Seen from an energy consumption perspective, control is not optimal. To make control more optimized energy-wise, while still retaining proper pressure control, the static pressure set point should be altered automatically, along a predefined path.

The developed simulation systems used as basis for this study cannot at this stage account for heating of air due to friction and throttling in the system. The error introduced by this is assessed not to be very significant due to other more dominant loads.

The following sections will explain the models and simulation systems used to demonstrate the possible benefits of the reset algorithm in practice. Furthermore, a case study will be carried out and discussed.

2. Procedure to reset of static pressure difference set point

The study presented in this section is based on (Sørensen 2011). Fig. 1 shows three different paths from one flow rate to another in the fan diagram. In this diagram, we consider pressure difference along the y-axis, and flow rate along the x-direction. Path 1-2 is the normal path to follow during constant fan pressure difference control. Pressure variations due to throttling in the duct system are then compensated for by adjusting the fan speed. Path 1-4 is obtained while there is no throttling going on in the duct system and thus no static pressure control is needed. This is the optimal path from an energy consumption perspective. Path 1-4 is used in a variable air volume ventilation system addressing a DDCV control strategy. Path 1-3 represents a compromise between path 1-2 and 1-4. This means more speed regulation and less throttling than 1-2. The path 1-3 was used in this study to reset the set point as a function flow rate.
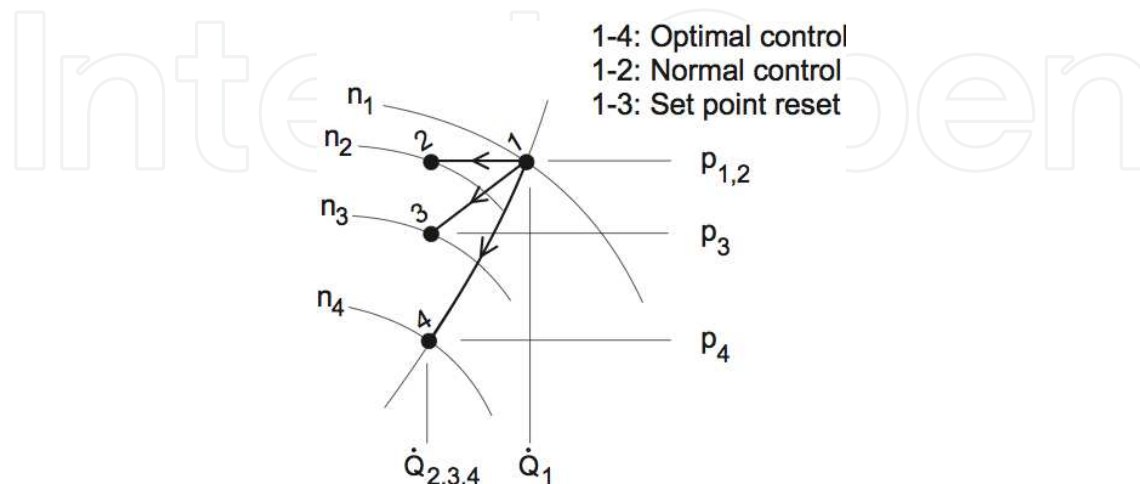

Figure 1. Three different paths of getting from one flow rate to another in the fan diagram (n=fan speed, Q=flow rate, p=pressure)

The direction of path 1-3 must be very carefully assessed. Choosing a too slack slew rate is not critical, but then there will be room for more energy savings still. Choosing a too steep curve is however critical. A too steep curve will affect the available maximum air flow rate for the local zones in the building. The risk of getting too little air to some zones is then present.

The algorithm for resetting the set point along path 1-3 is presented below. The following parameters have to be found or known:

- The set point to which the fan pressure difference normally would have been controlled - $\Delta p_{1,2}$.
- Design airflow rate (all local dampers open) - Q_1.
- Lowest airflow rate at $\Delta p_{1,2}$ (all local dampers closed) - $Q_{2,3,4}$. This will be the minimum flow rate from the fan during operation.
- Pressure difference at minimum fan speed (all local dampers open) - Δp_4.

The parameters can be found for instance during the commissioning process, by measurements or from the fan characteristics. In addition to these parameters, a gain (K_{path}) must be carefully selected. K_{path} determines the steepness of the path 1-3 (refer to Fig. 1) and is in the range between 0 and 1. A value of zero means no adjustment of the set point, and a value of one means nearly pure fan speed control. The reset algorithm was obtained through a linear curve fit of the above parameters, and requires continuous measurements of the main air flow rate:

$$\Delta p_{SP} = \Delta p_{1,2} + K_{path} \cdot \frac{\Delta p_{1,2} - \Delta p_4}{\dot{Q}_1 - \dot{Q}_{2,3,4}} \left(\dot{Q}(t) - \dot{Q}_1 \right) \tag{1}$$

To avoid that the set point moves to a very low or high value, it should be saturated at a maximum value. Stopping the set point from moving to a too high or too low value can be achieved by implementing the following algorithm in the controller:

if $\Delta p_{SP} > \Delta p_{1,2}$

then $\Delta p_{SP} = \Delta p_{1,2}$

if $\Delta p_{SP} < \Delta p_4 + (1-K_{path}) \cdot (\Delta p_{1,2} - \Delta p_4)$

then $\Delta p_{SP} = \Delta p_4 + (1-K_{path}) \cdot (\Delta p_{1,2} - \Delta p_4)$

3. Simulation system description

3.1. Fan model

The pressure and flow characteristics produced by the fan model, are crucial for the simulation results. Thus quite much effort has been put into the development of a proper fan model. The model is based on a backward curved, inclined radial fan, and takes into account fan efficiency and mechanical losses.

The model presented below refers to a fan which has no mechanical losses, which applies to incompressible flow and on which the mathematical description is purely based on the fan laws. Losses, in terms of fan efficiency, is added to the model later, thus enabling computation of the required fan power and energy usage and also the fraction of fan power which goes into heating of ventilated air.

For simulation of flow distribution throughout the ventilation system, a function which expresses the relationship between pressure difference, air flow rate and fan speed is required. This function can be derived, using a second order parabolic polynomial, as follows:

$$\frac{\Delta p_2}{\Delta p_1} = \left(\frac{n_2}{n_1}\right)^2 = \left(\frac{\dot{Q}_2}{\dot{Q}_1}\right)^2 = K_A \cdot \left(\frac{n_2}{n_1}\right)^2 + K_B \cdot \left(\frac{\dot{Q}_2}{\dot{Q}_1}\right)^2 + K_C \cdot \left(\frac{\dot{Q}_2}{\dot{Q}_1}\right) \cdot \left(\frac{n_2}{n_1}\right) \tag{2}$$

This relation is developed from the general polynomial model presented by (Lorenzetti, 1993). The factors K_A, K_B and K_C can be found by specifying certain boundary conditions of the fan characteristics. If assuming that the maximum pressure difference Δp_{max} is present at an air flow rate of Q_{pmax}, and that the maximum air flow rate Q_{max} is found at the minimum pressure difference (that is a pressure difference of zero), the boundary conditions of the characteristic are:

$$\Delta p_2 = \Delta p_{max} \qquad \text{for} \qquad Q_2 = Q_{pmax} \qquad \text{and} \qquad n_2 = n_{max}$$

$$\Delta p_2 = 0 \qquad \text{for} \qquad Q_2 = Q_{max} \qquad \text{and} \qquad n_2 = n_{max}$$

In addition, the following constraint must be fulfilled:

$$\left.\frac{\partial(\Delta p_2)}{\partial \dot{Q}_2}\right|_{n_2 = const} = 0 \quad \text{for} \quad Q_2 = Q_{pmax} \qquad \text{and} \qquad n_2 = n_{max}$$

Solving eq. NN for the factors K_A, K_B and K_C gives:

$$K_A = \frac{\Delta p_{max}}{\Delta p_1} \cdot \left(\frac{n_1}{n_{max}}\right)^2 \cdot \left(1 - \frac{\dot{Q}_{pmax}^2}{\left(\dot{Q}_{max} - \dot{Q}_{pmax}\right)^2}\right) \tag{3}$$

$$K_B = -\frac{\Delta p_{max}}{\Delta p_1} \cdot \left(\frac{\dot{Q}_1^2}{\left(\dot{Q}_{max} - \dot{Q}_{pmax}\right)^2}\right) \tag{4}$$

$$K_C = \frac{\Delta p_{max}}{\Delta p_1} \cdot \frac{n_1}{n_{max}} \cdot \frac{2 \cdot \dot{Q}_1 \cdot \dot{Q}_{pmax}}{\left(\dot{Q}_{max} - \dot{Q}_{pmax}\right)^2} \tag{5}$$

where for instance Δp_1, Q_1 and n_1 refer to the point at which Δp_{max}, Q_{pmax} and n_{max} occur. Hence, the governing (ideal) fan model can be expressed by:

$$\frac{\Delta p(t)}{\Delta p_{max}} = \left(\frac{n(t)}{n_{max}}\right)^2 - \left(\frac{\dot{Q}(t) - \dot{Q}_{pmax} \cdot \dfrac{n(t)}{n_{max}}}{\dot{Q}_{max} - \dot{Q}_{pmax}^{\;2}}\right)^2 \qquad (6)$$

Q_{max}, Q_{pmax} and n_{max} can be found from fan product catalogues.

The total efficiency of the fan must be known to compute the total fan power and energy usage. In this section, a simplified model of fan efficiency is presented.

It is based on the following assumption:

- Fan efficiency scale to the system pressure (or working) characteristic.

This means that if the flow obstacles in the ventilation system are kept unchanged, the fan efficiency is constant, even if the fan speed is altered. Note that since the mechanical losses are directly proportional to the fan speed, the total efficiency of the fan is not constant.

Below, the terms fan efficiency and total fan efficiency are addressed. For a VAV system in which the air flow is controlled by a fan only (a single zone system or a DDCV system), the fan efficiency is approximately constant. In more complex systems, control dampers and VAV boxes continuously change the flow resistance and hence the system pressure (or working) characteristics. Then the fan efficiency is a variable which depends on both the flow rate and the fan speed.

Fan efficiency can be modelled in a similar manner as the pressure drop shown earlier, using a second order polynomial to fit two arbitrary chosen data points from the fan characteristics; $\eta_1 = f(n_1, Q_1)$ and $\eta_2 = f(n_1, Q_2)$. The resulting expression for the fan efficiency then becomes:

$$\eta_f(t) = \frac{\eta_1 \cdot \dot{Q}_2^{\;2} - \eta_2 \cdot \dot{Q}_1^{\;2}}{\dot{Q}_1 \cdot \dot{Q}_2 \cdot \left(\dot{Q}_1 - \dot{Q}_2\right)} \cdot n_1 \cdot \frac{\dot{Q}(t)}{n(t)} - \frac{\eta_1 \cdot \dot{Q}_2 - \eta_2 \cdot \dot{Q}_1}{\dot{Q}_1 \cdot \dot{Q}_2 \cdot \left(\dot{Q}_1 - \dot{Q}_2\right)} \cdot n_1^{\;2} \cdot \left(\frac{\dot{Q}(t)}{n(t)}\right)^2 \qquad (7)$$

The total efficiency η_t at any speed n can be related to a reference mechanical efficiency $\eta_{mech,0}$ at a reference speed n_0 as follows (Eck, 1973):

$$\eta_t(t) = \frac{\eta_f(t) \cdot \eta_{mech,0}}{\eta_{mech,0} + (1 - \eta_{mech,0}) \cdot \left(\dfrac{n_0}{n(t)}\right)^2} \qquad (8)$$

Since fans are installed and connected to the air handling unit or ducts in different manners, entrance and discharge losses are normally not included in the fan efficiency.

Furthermore, to simulate fan acceleration, a rate limiter has been added to the relative speed input (i.e. input 2). The fan drive speed input is in itself equal to the controller output (or the frequency inverter output), and must be limited. Typical acceleration times for common HVAC fans are in the range of 5 - 20 sec (Daly, 1988).

3.2. Fan model validation

Most of the component models used in the study have been validated through comparison with either measurements or product data, and show good agreement with real life equipment. See for instance (Sørensen, 2006, 2008, 2010) for a complete overview.

The non dynamical qualities of the pressure/flow fan model were examined by comparing the model output with data from fan product catalogues (fan characteristics) Such comparisons was made for two non ducted real fans. Both were backward inclined radial fans, but of different size and capacity. Fig. 2 and Fig. 3 show comparisons of the output from the model and data from the real fan characteristic.
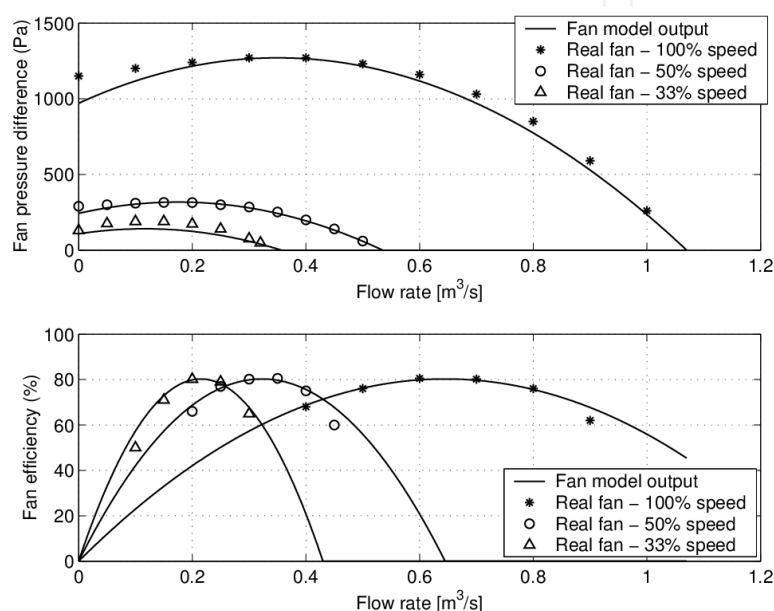
Figure 2. Comparison of pressure and flow rate produced by model to real fan data (small fan).
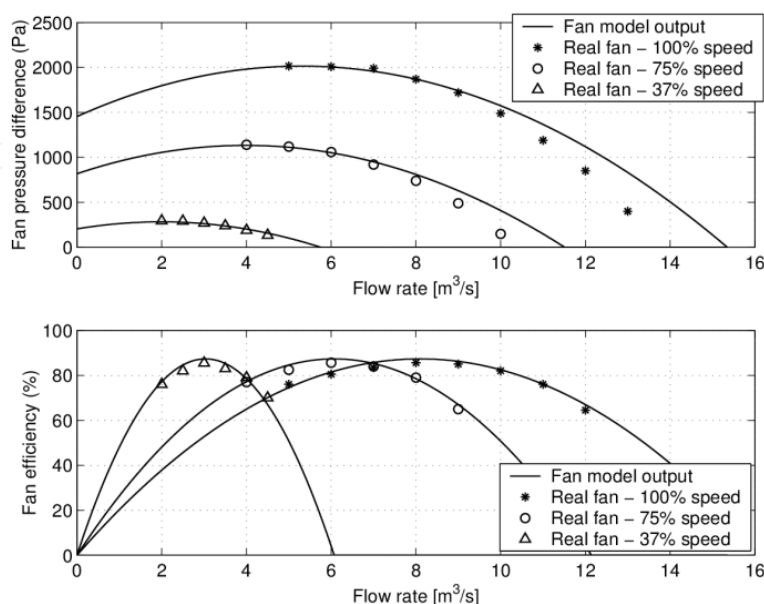
Figure 3. Comparison of pressure and flow rate produced by model to real fan data (large fan).

3.3. Simulation system

The study addressed a CO_2 controlled VAV system serving four similar classrooms in a school (Fig. 4).
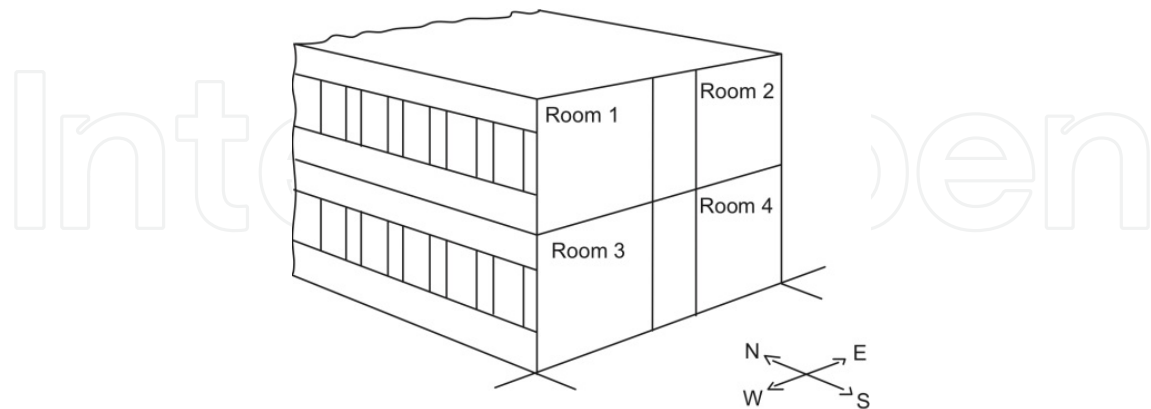

Figure 4. The investigated scenario; four classrooms in a school. Two rooms are facing west and two are facing east

The tool used for modeling and simulation was Matlab Simulink, developed by Mathworks. Matlab Simulink enables a visual programming technique, and is well suited for dynamic (time dependent) modeling. The program facilitates a modular approach, giving the user possibility to re-use models in other simulations.

The dynamic simulation system (Fig. 5) was built of four main subsystems:

- a steady state flow/pressure system
- a dynamical thermal building system
- a dynamical thermal air handling unit (AHU) system
- a dynamical contaminant building system.

The flow/pressure supply air subsystem is shown by Fig. 6. A steady state approach was chosen for the flow/pressure subsystem because changes to the parameters will have almost immediate effect on other connected subsystems. While for instance the thermal systems use considerable time to stabilize its outputs after a change on the inputs, the flow/pressure system outputs will change without any delay caused by inertia. The only dynamic elements of the flow/pressure subsystems are pure time delays caused by transportation of air in the ducts, time dependent ramp functions to model opening/closing time of dampers and ramp functions modulating fan speed.

Each of the blocks of Fig. 6 represents a component model describing the air flow and pressure loss through that component. To calculate pressure loss of ducts, duct fittings, dampers and so on, flow (velocity) dependent functions of friction and single loss factors have been implemented in the various component models. Flow rates are fed forward through the systems (from main duct to terminals), while pressures are summarized backwards. The total pressure loss is compared to the set point of the fan controller, and based on this, fan speed is either increased or decreased. This creates a simulation system

which has to be solved by iteration for each time step. The computed airflow rates from the pressure/flow system were fed into the other systems, and the room CO_2 and temperature responses were computed.
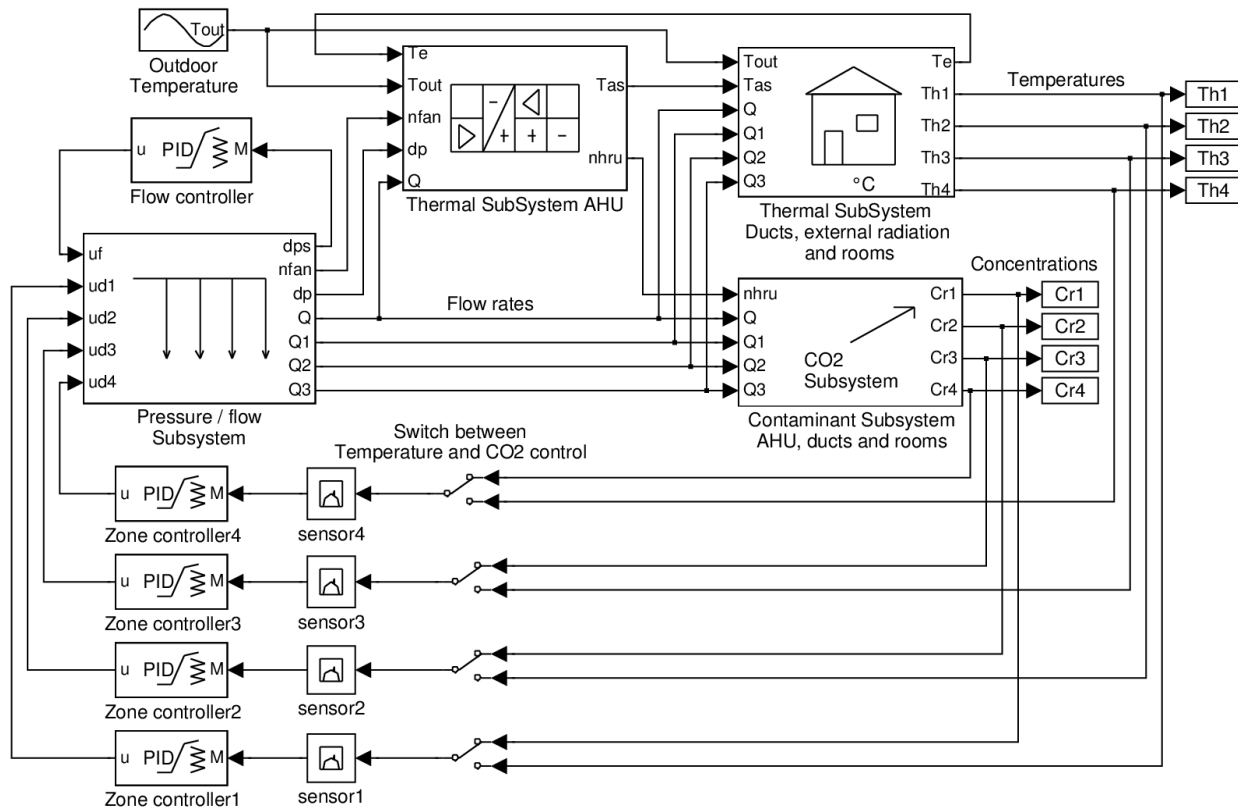

Figure 5. Main simulation system.

The thermal subsystem (AHU – air handling unit, ducts and rooms) was implemented to be able to calculate energy consumption from the dynamical system states. The AHU simulation subsystem, shown in Fig. 7, contains fan, water based heating coil, cooling coil and rotary heat recovery unit (HRU). It also contains thermal models for pipes, ducts, shunt, actuator and controls. Heating coil, het recovery unit and cooling coil are controlled by a sequential PID controller, which ensures that operation of these units is not overlapping. The sequence PID has three sets of controller parameters to ensure proper control of all the units.

The contaminant subsystem considers CO_2 room responses from human presence. The model is a simple dynamic mass balance of CO_2 in a room that accounts for infiltration/exfiltration, ventilation efficiency, and through a contaminant model of a rotary heat exchanger, also for leakage of exhaust air to the supply. Based on the supply air CO_2 concentration and the chosen set point of the rooms, flow rates will by varied. For instance, if room concentration is too high in a room, i.e. above set point, flow rate to the room will be increased until the concentration falls below the set point again. If concentration continues to fall, flow rate will be decreased accordingly. At zero occupancy, flow rate will decrease to a minimum level. For more details, refer to Sørensen 2006, 2008, 2010.
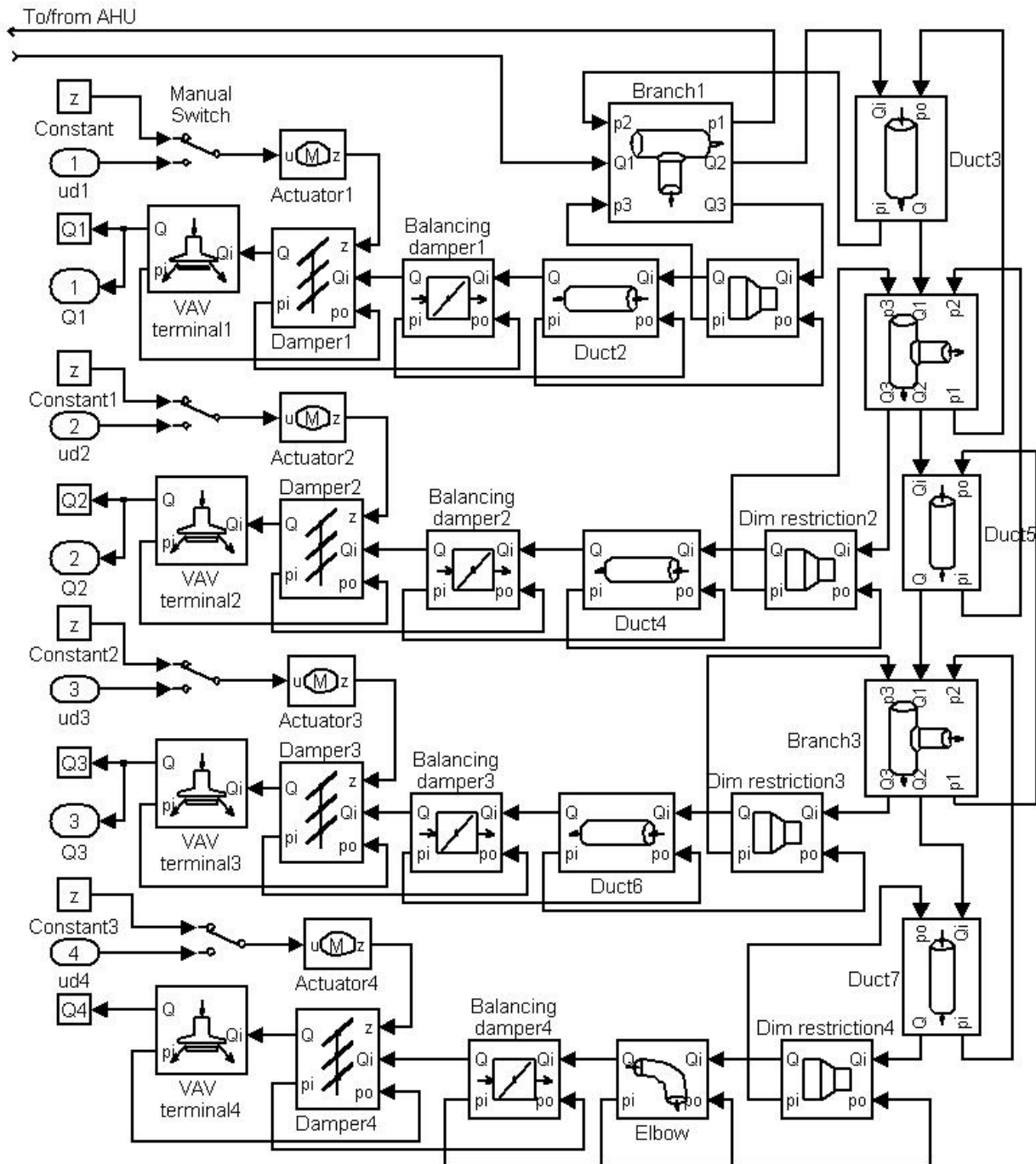
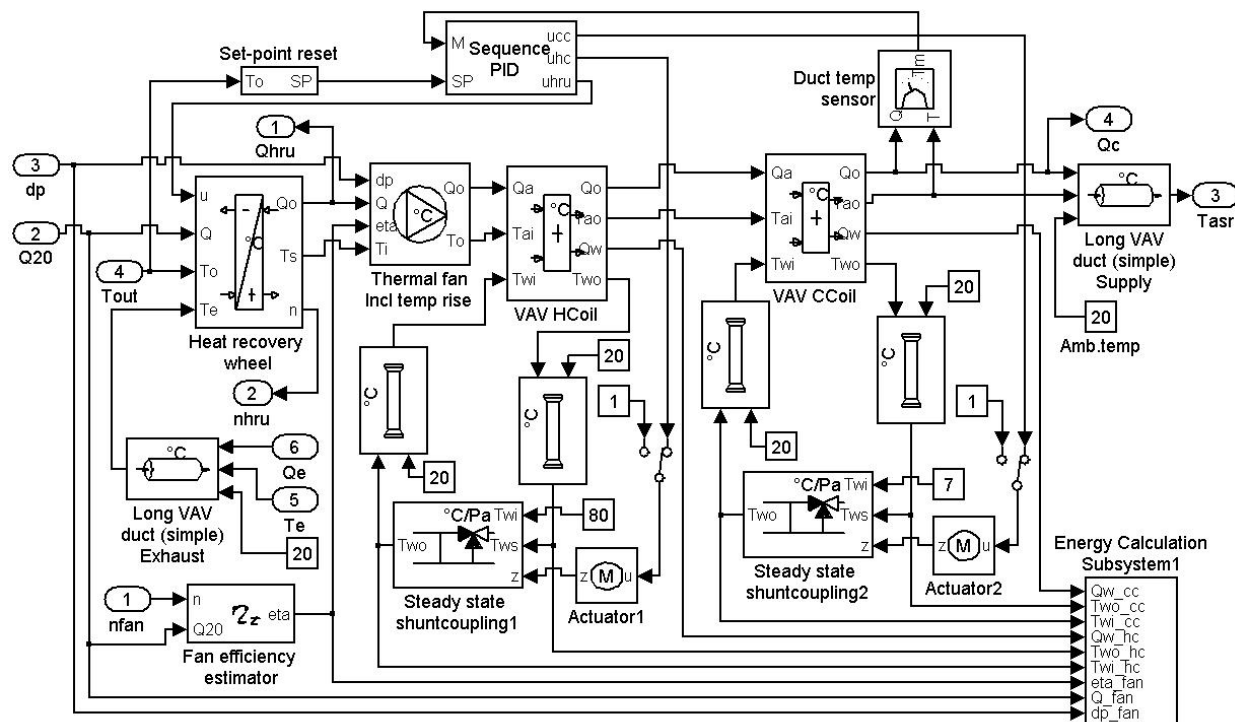**Figure 6.** The pressure/flow supply system model (steady state). Each block represents a component model.

Figure 7. Simulation model (block diagram) of the air handling unit model.

3.4. Case study

The ventilation system served four classrooms in a school. The ventilation system was designed for a maximum CO_2 level of 800 ppm, which approximately gives the same flow rate as mandated by the Norwegian building regulations. Minimum flow rates were determined from 2 liters/s per m^2 floor area. Design values rates for each room thus as follows:

- Maximum occupant load: 28
- Ventilation flow rate (m^3/h): 1150
- Minimum flow rate (m^3/h): 430
- Room volume (m^3): 180

Ventilation was turned on at 07.00, and shut down at 18.00. The main ducts and AHU were designed to handle 4600 m^3/h of air. Infiltration ratios were 0.1 air changes per hour. The maximum flow rate from the fan characteristic was 2.2 m^3/s and the pressure peak was 2100 Pa at 0.6 m^3/s. The HRU was sequentially controlled with water-to-air heating and cooling coils, using PID controllers. At design conditions, the heating coil was able to increase air temperature by 15°C, with supply and return water temperatures of 80 and 60° C. The cooling coil gave a maximum air temperature drop of -15°C at 7/13°C water temperatures.

Temperature efficiency of the HRU at design conditions was 60%. The HRU had a purge sector and the leakage factor was specified to 0.05 (Sørensen, Riise, 2010). It should be noted that the leakage was considered to be constant over the HRU, even though this may vary for a VAV system (Sørensen, 2008).

The outdoor CO_2 level was considered to be constant at 400 ppm. In all cases the occupant load varied as shown in Tab. 1. It was assumed that the time used by occupants to enter or leave the rooms was 5 seconds per occupant.

The building was considered to be multi storey, wherein the simulated rooms had only one exterior surface each. Moreover, terrain was assumed to be completely flat on the west side of the building. On the east side there was an obstruction of angle 20° in the two middle 45° view sectors (the 180° horizontal view from the windows was divided into four 45° sectors) (Sørensen, 2006). As shown in Fig. 2, classroom 1 and 2 were facing west and classroom 3 and 4 were facing east. There was no external shading. Windows were internally shaded (light curtains, 50% reflection) between hour 09.00 and 12.00 in classroom 2 and 4, and from 14.00 to 17.00 in classroom 1 and 3. Window U-value and solar factor were respectively 2.0 W/m^2K and 0.7. Total window area of each room was 9 m^2. The external wall had a U-value of 0.3 W/m^2K and a time constant of 15 hours. Internal walls, floor and ceiling had U-values of 0.7 W/m^2K and a time constant of 10 hours (light inner structure). Heat capacity of the interior was set to 10000 J/m^2K. The shares of radiation onto the walls from persons, internal equipment and external radiation (both atmospheric and solar) were respectively 0.5, 0.5 and 0.8. Heat from lights was specified to 10 W/m^2 and the lights were on between 07.00 and 18.00 only.

Hour of day	Room 1	Room 2	Room 3	Room 4
07.00	0	0	0	0
08.00	25	0	25	15
10.00	0	0	0	0
10.30	25	25	30	30
12.00	0	0	0	5
13.00	15	25	25	25
15.00	8	3	5	25
17.00	0	0	0	0
18.00	0	0	0	0

Table 1. Occupant load of selected four classrooms

4. Control strategy

Flow regulation was achieved through static pressure difference control of the fan and CO_2 control of the room airflow via local dampers. To account for steady state offset and to avoid too aggressive control, a PI controller was used on the fan. Pure P control was used locally. Maximum set point for the fan pressure difference control was 450 Pa. At this point the fan provided the design flow rate (at which the system was balanced and all local dampers were fully opened). To reduce throttling, and to ensure sufficient minimum flow rates to all zones, minimum damper positions were set to 30% of maximum. The correction gain of the

pressure set point (K_{path}) was calculated from a minimum flow rate of 0.8 m³/s at design pressure difference, and from a minimum pressure difference of 200 Pa. These values were chosen from the fan characteristics. Hence, the steady state paths of control were as shown in Fig. 8.

Room CO_2 set points were 700 ppm and supply air temperature was controlled between 15 and 18°C, dependent on outdoor temperature.
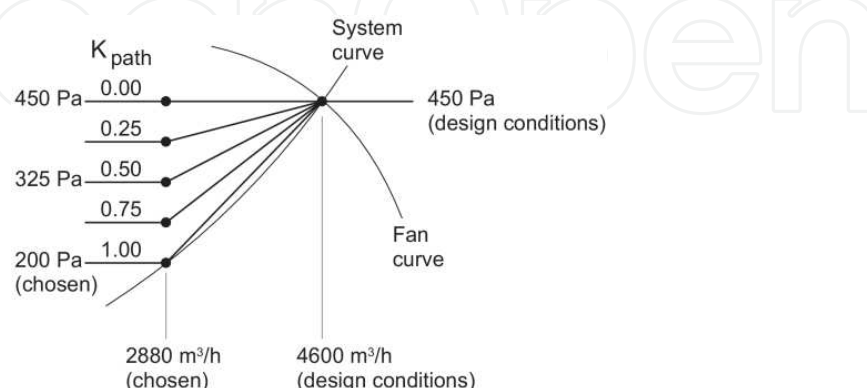

Figure 8. Paths of the pressure difference set point of the fan as a function of the correction gain K_{path}.

5. Results and discussion

Considering the limited data sets that were simulated, making any generalizations based on the simulation results in this case study would seem ambitious. The results are nevertheless important and can provide the basis for a more general representation of using variable set points on static pressure control.

Simulations were performed for different values of the gain K_{path} (0 to 1 with a step of 0.25). Three mean outdoor temperature levels were considered (-20, 0 and +20°C). Outdoor temperature varied as a ±4°C sinusoidal swing during a 24 hour period. Simulations included heat gain from solar radiation, and the simulated dates were in January, April, July and October. The energy consumption of 0°C outdoor conditions was determined as a mean between the usage of April and October.

The two upper diagrams of Fig. 9 show the pressure difference set points (left) and ventilation flow rates (right) during a day for different values of K_{path}. The remaining diagrams show how CO_2 responses in each of the rooms became for different values of K_{path}.

- Minimum flow rates to the zones decreased with an increasing K_{path}. However, due to a relatively wide minimum position on the dampers, all zones got a sufficient minimum flow rate (to maintain IAQ at no occupant load).
- For K_{path} approximately equal to 0.75, the flow rates to room 3 and 4 were marginally insufficient. The CO_2 level then rose slightly above the set point level (above the offset). It was at this point the maximum energy savings for this system were obtained.
- A K_{path} value equal to or below approximately 0.70 provided proper CO_2 control of all rooms.

- Although minimum flow rates were sufficient for a K_{path} of 1.0, the system was unable to provide enough air during occupancy. This shows in the CO_2 responses. It can be explained by first looking at a condition where all dampers are closed and secondly a condition where dampers are not closed. In the first case the fan delivers the minimum flow rate at 200 Pa pressure difference. The dampers are in their minimum positions (30% open). Then some dampers start to open, and as a result, the fan pressure difference drops. To compensate for the pressure drop, the fan increases speed to maintain the 200 Pa set point. The new flow rate is not sufficiently large to change the set point to a larger value (2880 m³/h). Thus, no changes in set point, even while the amount of air varied.
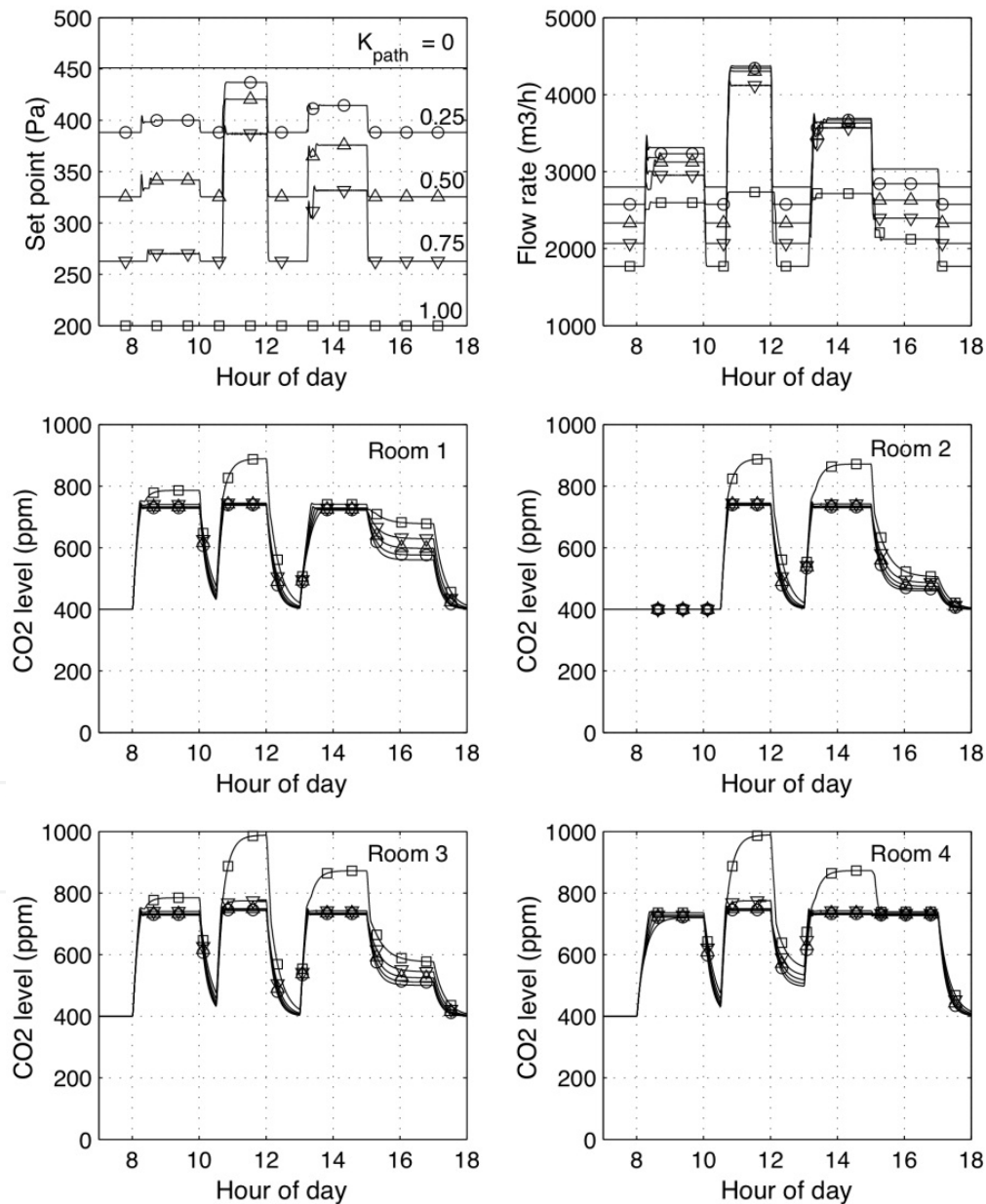

Figure 9. Simulation results of the system with pressure difference reset. The two upper diagrams show the SP and flow rate during a day. The remaining diagrams show CO_2 concentrations of the rooms.

In figure Fig. 10, the corresponding room temperature responses are shown for the different values of K_{path}. The effects from solar radiation on rooms with windows orientated in different directions can be seen here. Rooms with windows facing east naturally got high solar radiation early in the day, while windows facing west got high radiation later in the day. As flow rates were decreased, temperatures of course increased. Consequently, while deciding on a value of K_{path}, also thermal conditions should be assessed.
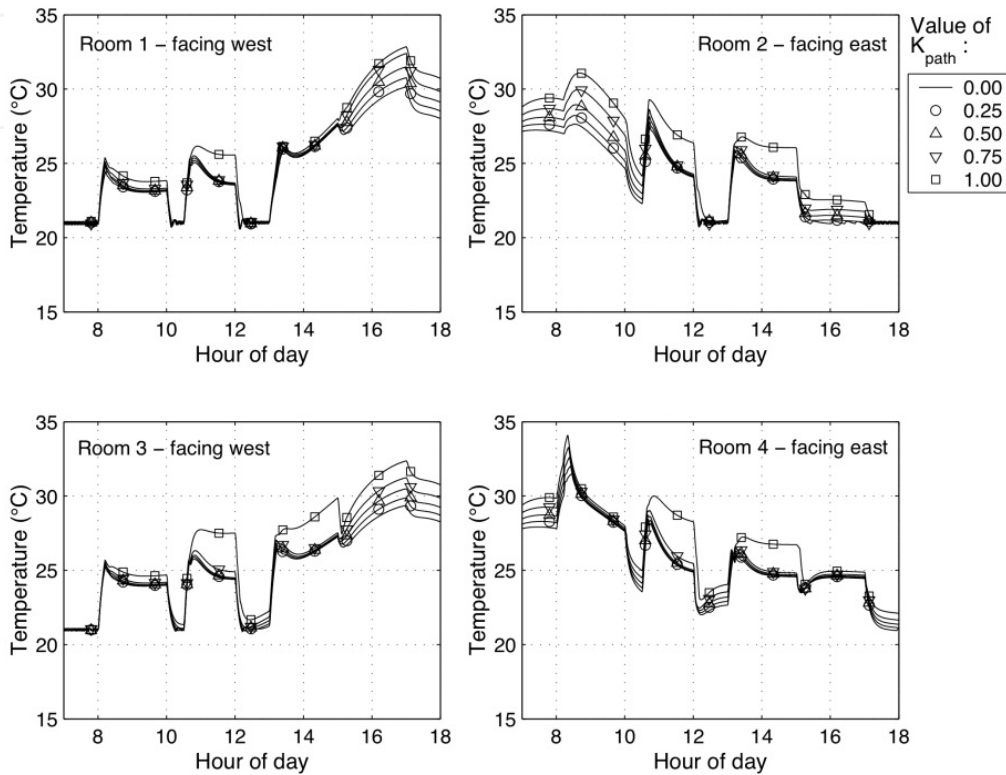

Figure 10. Room air temperatures during a day in July (+20°C outdoor temperature) in Narvik, Norway

Energy usage was compared to an identical VAV system with K_{path} gain equal to zero. In Fig. 11, percentage energy usage is shown as a function of K_{path}, for different outdoor temperatures. Energy usage was of course also affected by the degree of variation to the set point, i.e. the variation of K_{path}. The results generally indicate that energy usage for the AHU (and for the complete building) can be reduced considerably by utilizing variable set point control of the fan. The lack of integral function of the local zone controllers showed as a positive offset (up to 40 ppm). To account for the offset and to provide the correct flow rate to the rooms (specified in terms of a set point), the integral term should be utilized also for local control. In the simulations, the offset during full loads caused the flow rate never to reach design conditions.

Another important factor is damper authority. Low authority means that the dampers must produce a relatively high pressure drop before noticeably affecting flow rate. The dampers must then alter positions quite a bit to obtain the required flow regulation. In some cases this can lead to poor control and risk of instability, and will also affect flow rates to other rooms. Pressure independent VAV boxes represent a more sophisticated alternative. Other rooms are not affected to the same degree as for pure damper control. However, even these will suffer if damper authority is low.
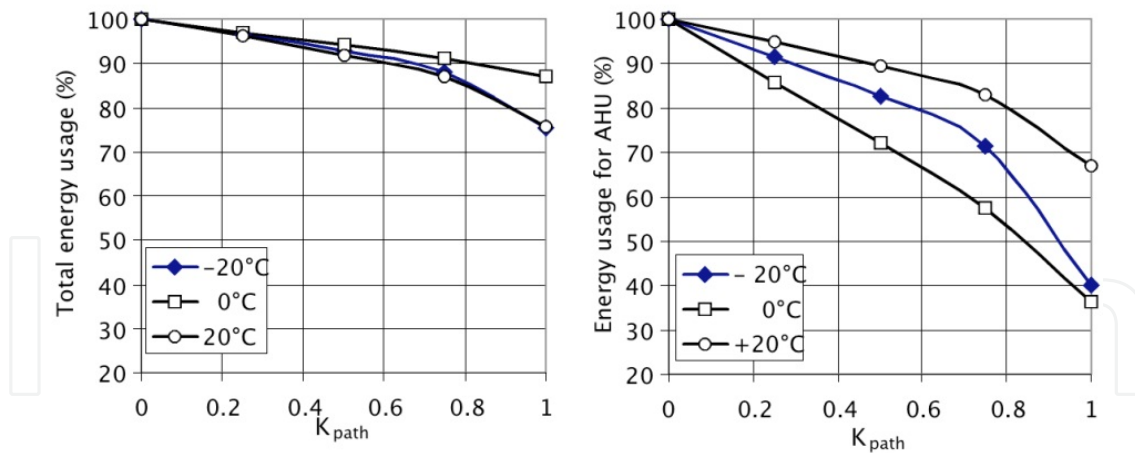
Figure 11. Energy usage (%) as a function of K_{path} and outdoor temperature (relative to a VAV system with K_{path} =0). The left diagram shows total energy usage (local heaters and lights included), and the right diagram shows energy usage for the AHU only. Location was Narvik, Northern Norway.

6. Conclusions

Reducing the energy consumption of the AHU using variable set point for control of fan pressure difference is possible. This study has suggested reductions up to 40% for the air conditioning process, as a result of implementing a more efficient control procedure for the fans. The main criteria to achieve this, is to choose the optimum value of K_{path}. Too low values will generate lower energy reductions. Too high values may lead to instability of the control loop, or no control at all. Influence on the results from other factors may also be important. The controller used for fan control is particularly important. Not so much which controller function that is addressed (P, PI or PID), but more how the controller parameters are determined. In this study, a PI controller was used on the fan, and parameters were determined from a modified Ziegler Nichols step response method. It was assumed that this gave fairly optimized control. It is likely that for larger ventilation systems using CO_2 DCV (or other types of DCV), the maximum value of the correction factor K_{path} (=0.7) will be lower than suggested in this case study, and other controller functions and parameters must be used to achieve the best possible results.

It is thus difficult to produce generalized numbers for K_{path}. The allowable level of correction of the set point must be found and assessed for each individual case.

Since the factor K_{path} obviously depends on occupancy, its maximum value will vary with the various load patterns that occur in the rooms, improved result can be obtained by adjusting it automatically. This can be done as follows (also refer to Fig. 12):

- The measured CO_2 concentrations (or any other control variables) in the rooms can be used as measures of inadequate control. A too large value of K_{path} will lead to augmented CO_2 levels above set point in the rooms. If levels are augmented, K_{path} is simply decreased by a controller.
- If concentrations can be maintained at the set points, K_{path} will be increased until concentrations starts to rise above set point.

Most commercial controllers allow for programming and are thus able to incorporate the algorithm presented above without major implications.
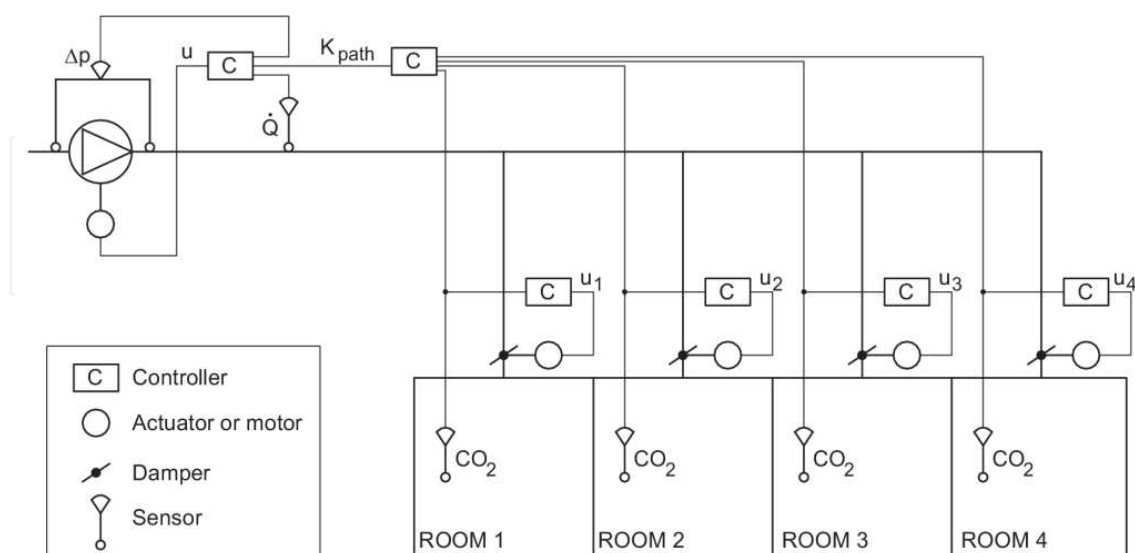

Figure 12. Fan static pressure difference control system (supply side only). The CO_2 concentrations of the zones (or exhaust) are used to determine the degree of set point variation (represented by K_{path}).

Author details

Bjørn R. Sørensen
Narvik University College, Norway

7. References

Daly, B. B. (1988). *Woods Practical Guide to Fan Engineering*. Woods of Colchester Limited.

Eck, B. (1973). *Fans: Design and Operation of Centrifugal, Axial-flow and Cross-flow Fans*. 1st English Edition, Pergamon Press, ISBN 0 08 015872 2.

Lorenzetti D. (1993). Modelling Adjustable Speed Drive Fans to Predict Energy savings in VAV Systems. *Proceedings of the 14th AIVC Conference*, Copenhagen, Denmark.

Sørensen, B. R. (2011). An Energy Efficient Control Strategy for Fan Static Pressure Difference, *Proceedings of the International Conference on Information Engineering and Mechanical Engineering (IEME)*, Xianning, China.

Sørensen, B. R. (2010). A Model Library for VAV Systems, *Proceedings of the 10th REHVA World Congress – Clima 2010*, Antalya, Turkey. ISBN 978-975-6907-14-6.

Sørensen, B. R., Riise, R. (2010). Rotary heat exchanger model for control and energy calculations. *Proceedings of AIVC 2010 conference*, Seoul, Korea.

Sørensen, B. R. (2008). Rotary heat exchangers and VAV systems. *Proceedings of the 11th international conference on indoor air quality - Indoor Air 2008*, Copenhagen, Denmark.

Sørensen, B. R. (2006) Demand Controlled Ventilation - A detailed study of energy usage by simulation. *Proceedings of the 27th annual AIVC conference*, Lyon, France.

Sørensen, B. R. (2006) Modelling and simulation of solar and atmospheric irradiation of Buildings. *Proceedings of the Cold Climate HVAC 2006*, Moscow, Russia.